Observation of Extremely Large Quadratic Susceptibility at 9.6–10.8 μm in Electric-Field-Biased AlGaAs Quantum Wells

M. M. Fejer, S. J. B. Yoo, and R. L. Byer
Edward L. Ginzton Laboratory, Stanford University, Stanford, California 94305

Alex Harwit[a] and J. S. Harris, Jr.
Stanford Electronics Laboratory, Stanford University, Stanford, California 94305
(Received 28 December 1988)

We have observed an extremely large second-order susceptibility for second-harmonic generation of 9.6–10.8-μm radiation due to intersubband transitions in electric-field-biased GaAs quantum wells. For 92-Å GaAs wells with 309-Å $Al_{0.48}Ga_{0.52}As$ barriers under a bias of 36 kV/cm, the peak value of the susceptibility was 28 nm/V, 73 times larger than for bulk GaAs. The magnitude and sign of the susceptibility depend on the bias field, and are in accord with theoretical predictions.

PACS numbers: 42.65.Ky, 73.20.Dx, 78.65.Fa

Transitions between the subbands of an isolated quantum well have extremely large oscillator strengths.[1] Strong infrared absorption features associated with transitions between the lowest two subbands in a GaAs quantum well have been observed by several groups.[1-3] Since nth-order nonlinear susceptibilities are proportional to the product of $n+1$ dipole matrix elements, strong nonlinear effects can also be expected.[4-7] As even-order susceptibilities vanish in structures with inversion symmetry, finite second-order susceptibilities can only be observed if the symmetry of the conduction-band potential is broken through either the growth of an asymmetric well or the application of an external bias field. We report here on the first measurement of the second-order susceptibility of a quantum well biased with an external field. The measurements of electric-field-induced second-harmonic generation of the 9.6–10.8-μm output of a CO_2 laser in modulation-doped AlGaAs quantum wells are in accord with theoretical predictions.

To calculate the nonlinear susceptibilities, we need the energy eigenvalues and dipole matrix elements for an electron in a quantum well under an applied electric field. The wave function is the product of a Bloch function, a plane wave in the plane normal to the layers ($\perp\hat{\mathbf{z}}$), and an envelope function ψ that depends only on z. Assuming vertical transitions between the subbands and unity overlap of the Bloch functions,[1] we need only consider the dipole matrix elements and energies of the envelope functions. The expression for the nonlinear polarizability for second-harmonic generation $\alpha^{(2)}$ is then the same as that given in Ref. 8 for transitions between discrete states,

$$\alpha_{33}^{(2)}=\frac{2e^3}{\epsilon_0\hbar^2}\sum_{mn}\langle z_{1n}\rangle\langle z_{nm}\rangle\langle z_{m1}\rangle\{[(\omega-\Omega_{n1}-i\gamma_{n1})(2\omega-\Omega_{m1}-i\gamma_{m1})]^{-1}+[(\omega+\Omega_{n1}-i\gamma_{n1})(2\omega+\Omega_{m1}-i\gamma_{m1})]^{-1}$$
$$-(2\omega-\Omega_{mn}-i\gamma_{mn})^{-1}[(\omega-\Omega_{m1}-i\gamma_{m1})^{-1}+(\omega+\Omega_{n1}-i\gamma_{n1})^{-1}]\}, \quad (1)$$

where $\langle z_{ij}\rangle=\langle\psi_i|z|\psi_j\rangle$, $\Omega_{ij}=(E_i-E_j)/\hbar$, $1/\gamma_{ij}$ is the dephasing time, and e is the magnitude of the electronic charge. We have assumed that only the lowest subband is thermally populated. In the low-density limit, the nonlinear susceptibility $\chi^{(2)}$ is given by $\chi^{(2)}=N\alpha^{(2)}$, where N is the number density of conduction electrons. Since at least one of the matrix elements in each term vanishes if the states are of definite parity, the magnitude of the nonlinearity depends strongly on those matrix elements, forbidden at zero field, that are induced by the bias field.

For a well of depth U_0 and width L centered at $z=0$, under a bias electric field $F\hat{\mathbf{z}}$ normal to the well, the envelope function ψ_n obeys $H(z)\psi_n=E_n\psi_n$, where we take the effective-mass Hamiltonian to be

$$H(z)=-\frac{\hbar^2}{2}\frac{d}{dz}\frac{1}{m(z)}\frac{d}{dz}+U(z)+eFz. \quad (2)$$

For $|z|<L/2$, $U(z)=0$ and the effective mass $m_e(z)=m_w$, while for $|z|>L/2$, $U(z)=U_0$ and $m_e(z)=m_b$. While the Schrödinger equation obtained with this Hamiltonian is readily solved numerically, insight into the effects of the bias field on the optical properties of the system can be obtained from an approximate solution of the infinite-well ($U_0\rightarrow\infty$) model. For this analysis, it is useful to introduce a characteristic confinement energy,

$E_0 \equiv \pi^2\hbar^2/2m_wL^2$, and a dimensionless measure of the strength of the bias field, $\Phi \equiv eFL/\pi E_0$. For the range of bias fields applied in this experiment, it is adequate to treat the electric field as a perturbation. In this case, we can obtain wave functions correct to first order in Φ [9]:

$$\psi_n(z) = \left(\frac{2}{L}\right)^{1/2}\left\{\cos(n\zeta) + \frac{\Phi}{4n}\left[(-1)^n\left(\frac{\pi^2}{4} - \zeta^2\right)\sin(n\zeta) + \frac{\zeta}{n}\cos(n\zeta)\right]\right\} \tag{3}$$

for n odd, and the same expression with cos and sin interchanged for n even. $\zeta \equiv \pi z/L$ is a dimensionless length. The energy eigenvalues accurate to second order in Φ are

$$\frac{E_n}{E_0} = n^2 + \Phi^2\frac{\pi^2}{48n^2}\left(1 - \frac{15}{\pi^2n^2}\right). \tag{4}$$

The dipole matrix elements are necessary for the calculation of the optical properties of the quantum well. The allowed matrix elements in a symmetric square well, i.e., those between states of opposite parity, have been given previously as [1]

$$\frac{\langle z_{mn}\rangle}{L} = (-1)^{(n+m+1)/2}\frac{8}{\pi^2}\frac{mn}{(m^2-n^2)^2}, \tag{5}$$

where we have neglected a correction proportional to Φ^2. From Eq. (3) we can obtain the dipole matrix elements that are disallowed at zero field, i.e., those between states of the same parity: for $m = n$,

$$\frac{\langle z_{nn}\rangle}{L} = \Phi\frac{\pi^2n^2 - 15}{24\pi n^4}; \tag{6a}$$

for m,n odd,

$$\frac{\langle z_{mn}\rangle}{L} = \Phi\frac{(-1)^{(n+m)/2}}{\pi}\frac{m^2+n^2}{nm(m^2-n^2)^2}, \tag{6b}$$

and the negative of the latter expression for m,n even. Despite the derivation of Eqs. (3) and (4) as expansions in powers of Φ, the dipole matrix elements calculated with Eqs. (5) and (6) agree to within several percent with numerical calculations for Φ on the order of 1 (fields of 200 kV/cm for a 92-Å GaAs well). [10]

For wells of finite depth, the wave function spreads into the barrier region, and the above analysis is no longer valid. For the purpose of discussion, it is adequate to use the effective-width approximation, [11] where we replace L in the expressions for the infinite well with L_e, where L_e is chosen to yield the correct ground-state energy for the finite well at zero bias. For a 92-Å GaAs well, with $Al_{0.48}Ga_{0.52}As$ barriers, we take the material parameters at 80 K to be $m_w = 0.067m_0$, $m_b = 0.107 \times m_0$, [12] the direct-bandgap energy $E_{g,w} = 1.507$ eV in the well [13] and $E_{g,b} = 2.163$ eV in the barrier, [12,14] and the conduction-band discontinuity as $0.63(E_{g,b} - E_{g,w})$. [15] With these parameters, we find that the ground-state energy of the unbiased well is 38 meV, resulting in an effective width of $L_e = 122$ Å. The quantities of interest for the calculation of optical properties can then be obtained by scaling the infinite-well results by $L_e/L = 1.32$. These scaled values, followed by the results from numerical solutions, are $E_1 = 38$ (38) meV, $E_2 = 152$ (152) meV, $E_3 = 342$ (332) meV, $\langle z_{12}\rangle = 22$ (22) Å, $\langle z_{23}\rangle = -24$ (−24) Å. For a bias field of 36 kV/cm, we find $\langle z_{13}\rangle = 0.74$ (0.74) Å, $\langle z_{11}\rangle - \langle z_{22}\rangle = -3.9$ (−3.7).

With Eqs. (5) and (6) for the dipole matrix elements and Eq. (4) for the eigenvalues, we can evaluate Eq. (1) for the nonlinear susceptibility. Consider a well with three bound states. The peak in the nonlinear susceptibility at $2\omega = \Omega_{31}$ ($\hbar\omega = 152$ meV for our example) is dominated by the $n = 2$, $m = 3$ term of Eq. (1). Considering only this term, we have with Eqs. (4) and (6)

$$\alpha^{(2)}(\omega = \Omega_{31}/2) \approx i\frac{1024}{45\pi^2}\frac{e^4}{\epsilon_0\hbar}\frac{F}{m_w^2\gamma_{31}\omega^4}. \tag{7}$$

Taking $N = 5\times10^{17}$ cm^{-3}, $\hbar\gamma_{13} = 7.5$ meV, and $F = 36$ kV/cm, we find $N\alpha^{(2)}(2\omega = \Omega_{31}) = 2.4\times10^{-8}$ m/V. For comparison, the nonlinear susceptibility of bulk GaAs, a highly nonlinear material, is $\chi_{14}^{(2)} = 3.8\times10^{-10}$ m/V. [16] From Eq. (7) it can be seen that the nonlinearity is inversely proportional to the square of the effective mass of electrons in GaAs, reflecting the fact that the size of a quantum well in resonance with a photon of a given energy increases with decreasing effective mass. The nonlinear susceptibility is also inversely proportional to the linewidth of the resonant transition. The magnitude of the discontinuity in the conduction band does not appear in the expression, as might be expected in the effective-width approximation. Finally, we note that the magnitude and sign of the nonlinear susceptibility are proportional to the applied bias field.

While the simple Hamiltonian in Eq. (2) is useful for a qualitative discussion of the nonlinear susceptibility, the nonparabolicity of the conduction band must be included in quantitative calculations. [17] We approximate the nonparabolicity with an energy-dependent effective mass defined by $\hbar^2k^2/2m(E) = E(k)$, chosen to agree with the quartic dispersion relation for GaAs given in Ref. 12. The reduction in the energy of the eigenstates caused by the nonparabolicity affects the magnitude of $\alpha^{(2)}$ both by shifting the location of the resonances, and by reducing the magnitude of the dipole matrix elements by reducing the barrier penetration of the wave functions. For our 92-Å example, E_3 shifts by 42 meV, significantly reducing the separation of Ω_{21} and $\Omega_{31}/2$, approximately doubling $\alpha^{(2)}(\omega = \Omega_{31}/2)$.

The magnitude of the intersubband nonlinearity can

be obtained experimentally from a measurement of electric-field-induced second-harmonic generation. We used a sample grown by molecular-beam epitaxy in a Varian Gen-II system. A 0.5-μm, $n=2\times10^{17}$-cm^{-3}-doped GaAs buffer layer followed by fifty periods of the superlattice was grown on a 500-μm, $n=7\times10^{16}$-cm^{-3}-doped substrate. A period of the superlattice consists of a 309-Å $Al_{0.48}Ga_{0.52}As$ barrier and a nominally 92-Å GaAs well. The center 132 Å of the barrier is doped at 6×10^{17} cm^{-3}, while the well is undoped. The structure is capped with a 1.3-μm GaAs layer, the first 500 Å of which is doped at 1×10^{18} cm^{-3}, the next 0.75 μm at 2×10^{17} cm^{-3}, and the top 0.5 μm at 2×10^{18} cm^{-3}. The dopant in all layers is silicon.

The sample was first characterized by infrared absorption measurements on a Digilab FTS-40 Fourier-transform infrared spectrometer. The wafer was oriented at Brewster's angle in a beam polarized in the plane of incidence. At 80 K an absorption line was observed at 112 meV with FWHM of 5 meV. The integrated absorption strength was 0.50 as large as predicted from the theoretical oscillator strength, which is accounted for in the remainder of the calculations by using a similarly reduced effective doping density. Measurements of the much weaker absorption of the 1-3 transition have not yet been obtained.

The transition energies and dipole matrix elements were calculated by numerical solution of Eq. (1) with a quartic dispersion relation, including a first-order perturbation calculation of the energy shift due to band bending. The macroscopic susceptibilities, related to the polarization $\mathcal{P}^{2\omega}$ by $\langle\mathcal{P}^{2\omega}\rangle=\chi^{(1)}\langle E^{2\omega}\rangle+\chi^{(2)}\langle E^{\omega}\rangle^2$, where the angular brackets indicate averaging over one period of the structure, were calculated in a self-consistent field approximation[18] carried out to second order in the applied fields. Many-body effects were neglected, and the numerical calculation was simplified by neglecting coupling of the different subband transitions. The major differences between this calculation and the simple result $\chi^{(2)}\approx Nf\alpha^{(2)}$, where f is the fraction of the structure filled by the quantum wells, are a blue shift of the resonances, and an overall reduction in the magnitude due to the difference between the bulk linear susceptibilities of the well and barrier. The magnitude of the second-order susceptibility for $F=36$ kV/cm, calculated with the empirical values for Ω_{21} and γ_{21}, the theoretical value for Ω_{31}, and $\hbar\gamma_{31}=7.5$ meV, is plotted versus fundamental frequency in Fig. 1.

The harmonic generation measurements were made with a grating-tuned, rotating-mirror, Q-switched CO_2 laser focused to a spot of approximately 50 μm diameter at the sample. The laser output was typically a train of 200-ns-long pulses with a peak power of 1 kW and a 100-Hz repetition rate. The bias voltage was applied every other laser pulse, and the second-harmonic output was monitored with a boxcar integrator operated in an active baseline-subtraction mode, so that only the portion

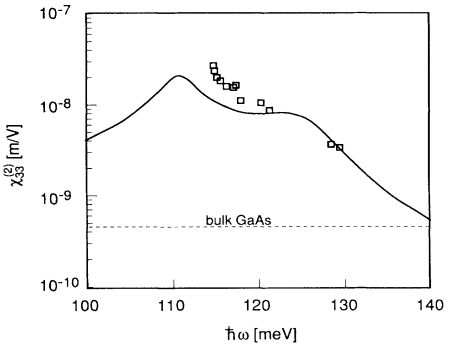

FIG. 1. Calculated nonlinear susceptibility for second-harmonic generation $\chi^{(2)}$ as a function of the energy of the fundamental photon. Squares are experimental measurements.

of the second-harmonic radiation that depended on the applied voltage was measured.

The total second-harmonic output is the coherent sum of the contributions from the quantum-well layer and the substrate. For a fundamental beam propagating at an angle θ to $\hat{\mathbf{z}}$, it can be shown that the total second-harmonic power generated in the sample $P_{2\omega}$ is given by

$$P_{2\omega}\propto P_{\omega}^2\,|\,A\chi_{33}^{(2)}+B\chi_{14}^{(2)}[\cos(\theta)\phi-t\gamma]\,|^2, \tag{8}$$

where A and B are possibly complex geometry-dependent factors, t is the ratio of the transmission coefficients for radiation polarized normal and parallel to the plane of incidence, and $\chi_{14}^{(2)}$ is the nonlinear susceptibility of bulk GaAs. ϕ, the angle between a [100] axis of the crystal and the intersection of the plane of incidence with the surface of the wafer, and γ, the angle between the fundamental electric field and the plane of incidence, are assumed to be small. As can be seen from Eq. (7), to first order $\chi_{33}^{(2)}$ is proportional to the applied bias field F. It is then clear from Eq. (8) that $P_{2\omega}$ is a quadratic function of the bias voltage V and that the minimum of the parabola shifts linearly with ϕ and γ.

$P_{2\omega}$ was measured for several wavelengths as a function of V at $\phi=\gamma=0$. The expected parabolic dependence is obeyed, with wavelength-dependent curvature reflecting the dispersion of $\chi_{33}^{(2)}$. The minima of the parabolas fall at $V=V_0\approx3$ V, rather that at $V=0$ as predicted by Eq. (8). That V_0 is the same for all the wavelengths suggests that the shift is a result of built-in asymmetry in the well, rather than misorientation of the sample or imperfect polarizers. We note that measurements of the quadratic Stark shift of the 1-2 transition showed a similar offset.[19] Repeating the measurement of $P_{2\omega}$ vs V for several values of γ at a fixed wavelength showed a linear dependence of V_0 on γ, as predicted by Eq. (8). For fundamental wavelengths close to the absorption peak, deviations from the parabolic dependence of $P_{2\omega}$ vs V, attributed to the Stark shift of the peak, were observed at high bias fields.

To extract an absolute value for $\chi_{33}^{(2)}$, $P_{2\omega}$ was normalized to the second-harmonic power generated at room temperature in a 110-μm-thick undoped GaAs plate mounted in the same apparatus. The connection of the second-harmonic generation in the quantum-well layer to the nonlinear susceptibility is complicated by the resonant birefringence and dichroism, and the subwavelength thickness of the layer.[20] The linear index of refraction data necessary for the calculation were estimated from a Lorentzian model fitted to the absorption spectrum. The experimental values for $\chi_{33}^{(2)}$ plotted in Fig. 1 are obtained at $F=36$ kV/cm. The agreement between the experimental data and the model is reasonable in view of the uncertainty in the device parameters and AlGaAs material properties, the unknown energy and linewidth of the 1-3 transition, and the neglect of many-body effects.

The largest value of $\chi^{(2)}$, measured at a fundamental wavelength of 10.8 μm, is 28 nm/V, 73 times larger than for bulk GaAs. This susceptibility is among the highest measured for any material, and is typical of the large second- and third-order effects, e.g., sum and difference frequency generation, electro-optic modulation, dc and optical Kerr effect, that can be expected in intersubband transitions. The control of the sign and magnitude of $\chi^{(2)}$ through the bias electric field suggests novel device geometries; e.g., a periodic bias electrode could be used to induce a periodic sign alternation in $\chi^{(2)}$ for quasi-phase-matching nonlinear interactions.[21] The utility of these nonlinearities for most optical devices, especially those involving nonlinear frequency conversion, will depend largely on the ratio of the pertinent nonlinearity to the absorption coefficients, which could be considerably improved by working in the vicinity of a weakly allowed transition well separated from the allowed transitions. More complete data on the absorption spectra and material parameters are necessary for the evaluation of the potential of these structures for device applications.

The authors thank Eric Hellman for many helpful discussions, and acknowledge the support of the Air Force Office of Scientific Research through Contract No. AFOSR-88-0354 and the Joint Services Electronics Program through Contract No. N00014-84-K-0327.

[a]Currently at IBM Thomas J. Watson Research Laboratory, Yorktown Heights, NY 10598.

[1]L. C. West and S. J. Eglash, Appl. Phys. Lett. **46**, 1156 (1985).

[2]B. F. Levine, R. J. Malik, J. Walker, K. K. Choi, C. G. Bethea, D. A. Kleinman, and J. M. Vandenberg, Appl. Phys. Lett. **50**, 273 (1987).

[3]Alex Harwit and J. S. Harris, Jr., Appl. Phys. Lett. **50**, 685 (1987).

[4]L. C. West, Ph.D. dissertation, Stanford University, 1985 (unpublished).

[5]M. K. Gurnick and T. A. DeTemple, IEEE J. Quantum Electron. **19**, 791 (1983).

[6]S. J. B. Yoo, M. M. Fejer, Alex Harwit, R. L. Byer, J. S. Harris, Jr., J. Opt. Sci. Am. A **4**, 27 (1987).

[7]L. Tsang, D. Ahn, and S. L. Chuang, Appl. Phys. Lett. **52**, 697 (1988).

[8]Y. R. Shen, *The principles of Nonlinear Optics* (Wiley, New York, 1984), Chap. 2.

[9]L. I. Schiff, *Quantum Mechanics* (McGraw-Hill, New York, 1968), p. 263.

[10]Note that by symmetry the only second-order correction to the dipole matrix elements between states of the same parity is in the normalization constant, which, to second order in Φ, is $(2/L)^{1/2}C_n$, where $C_n^{-2}\equiv 1+\Phi^2\frac{1}{960}n^{-6}(2\pi^4n^4+5\pi^2n^2-210)$.

[11]D. A. B. Miller, D. S. Chemla, T. C. Damen, A. C. Gossard, W. Weigmann, T. H. Wood, and C. A. Burrus, Phys. Rev. B **32**, 1043 (1985).

[12]S. Adachi, J. Appl. Phys. **58**, R1 (1985).

[13]J. S. Blakemore, J. Appl. Phys. **53**, R123 (1982).

[14]D. E. Aspnes, S. M. Kelso, R. A. Logan, and R. Bhat, J. Appl. Phys. **60**, 754 (1986).

[15]M. Nakayama, H. Kuwahara, H. Kato, and K. Kubota, Appl. Phys. Lett. **51**, 1741 (1987).

[16]*Handbook of Lasers,* edited by R. J. Pressley (Chemical Rubber Co., Cleveland, 1971), p. 504.

[17]T. Hiroshima and R. Lang, Appl. Phys. Lett. **49**, 456 (1986).

[18]S. J. Allen, Jr., D. C. Tsui, and B. Vinter, Solid State Commun. **20**, 425 (1976).

[19]Alex Harwit, Ph.D. dissertation, Stanford University, 1987 (unpublished).

[20]D. Chemla and P. Kupecek, Rev. Phys. Appl. **6**, 31 (1971).

[21]K. C. Rustagi, S. C. Mehandale, and S. Meenakshi, IEEE J. Quantum Electron. **18**, 1029 (1982).